Transient and Persistent Spectral Hole-Burning in the R-lines of Chromium(III) in $NaMgAl(Oxalate)_3 \cdot 9H_2O$

Matthew L. Lewis and Hans Riesen*

School of Chemistry, University College, The University of New South Wales, Australian Defence Force Academy, Canberra, ACT 2600, Australia

Received: April 1, 2002; In Final Form: June 10, 2002

The temperature dependence of transient and persistent spectral holes is reported for the R-lines ($^2E \leftarrow {}^4A_2$ transitions) in 4% chromium(III) doped $NaMgAl(oxalate)_3 \cdot 9H_2O$. The temperature dependence is well described by taking into account two pseudolocal vibrations in a weak electron−phonon coupling model and the direct process between the two ^2E levels. The persistent spectral hole-burning is based on a *nonphotochemical* mechanism involving mainly a rearrangement of a water molecule of crystallization. The 1.12 GHz width of the transient hole in the R_2 line provides a value for the relaxation rate within the ^2E multiplet, $k(R_2 \rightarrow R_1) = 3.5 \times 10^9\ s^{-1}$ at 2.5 K. The observed optical line width of $\Gamma = 46$ MHz for the R_1-line at 2.5 K is most likely dominated by chromium(III)−chromium(III) spin−spin interactions. Spectral diffusion on the ms time scale causes *persistent* spectral holes to be significantly broader and holewidths of 260 MHz and 1.63 GHz for the R_1 and R_2-line, respectively, are observed. Spontaneous hole-filling is thermally activated and spectral diffusion on the minute time scale is slow in the investigated temperature range of 2.5−30 K.

1. Introduction

Optical transitions in condensed phases invariably suffer from inhomogeneous broadening and valuable information regarding the electronic structure is obscured.[1−6] Optical transitions are broadened by the variation of local fields. Laser techniques such as fluorescence line narrowing (FLN)[2] and spectral hole-burning[1] can overcome some aspects of this broadening. Subtle details can be explored by spectral hole-burning and this technique has been applied to investigate a wide range of problems.[1−6] Potential applications in optical storage devices prevail to be one of the driving forces behind many hole-burning studies.[1]

Although the phenomena of persistent[7,8] and transient[9] spectral hole-burning in the solid state were discovered almost 30 years ago, the number of crystalline systems for which *both* effects have been reported is limited.[10,11] The present paper reports on transient and nonphotochemical persistent spectral hole-burning in $NaMgAl(oxalate)_3 \cdot 9H_2O$:Cr(III). Nonphotochemical hole-burning is a common phenomenon in amorphous solids but rarely observed in crystalline systems.[12−15] NPHB can occur upon selective excitation of a subset of chromophores by minute variations of host−guest interactions.[1,16,17] For example, the hydrogen bonds between the host and the guest can be rearranged upon photoexcitation leading to a shift of the transition energy of the selected chromophores. NPHB in amorphous systems is usually described by the so-called two-level systems (TLSs).[1,16,17] The reported NPHB mechanisms in crystalline systems have been assigned to light-induced rearrangements of ions.[12−15]

Some early work reported the polarized absorption and emission spectra of $NaMgAl(ox)_3 \cdot 9H_2O$:Cr(III).[18−20] These studies were complemented by single-crystal EPR[21] and magnetic susceptibility[22] experiments on the $^4A_2$ ground state. The crystal structure originally reported by Frossard[23] was reinvestigated by Mortensen.[19] The space group was reported to be either $P3c1$ or $P\bar{3}c1$ with six formula units per unit cell. This is in agreement with the findings of EPR measurements: there are six magnetically inequivalent chromium(III) sites composed of two sets of three, each set being rotated from the other by 17.7°about the *c* axis. Furthermore, it was reported that the distortion from axial symmetry arises through the presence of one molecule of water of hydration for each $[Cr(ox)_3]^{3-}$ complex. Upon removal of this water molecule, the Cr(III) EPR and the ^{27}Al NMR spectra become axial.[21,24] It was postulated that the ease of reversibility of the water removal is due to the presence of channels within the crystal structure.[21]

TABLE 1: Results of Elemental Analysis

	% found	% calc $8H_2O$	% calc $9H_2O$	% calc $10H_2O$
hydrogen	3.66[a], 3.64[a], 3.61[b], 3.47[b]	3.34	3.63	3.89
carbon	14.45[a], 14.52[a], 14.43[b], 14.35[b]	14.94	14.40	13.90

[a] Ref 18. [b] This work; analysis performed by the Microanalytical Unit of The Research School of Chemistry, The Australian National University.

Recently, the crystal structure was redetermined and the space group was refined to $P\bar{3}c1$.[25] On the basis of the space group it was concluded that there are 10 molecules of water of crystallization. Elemental analysis has been performed by several groups,[18,21] and it was found that there are *nine* water molecules of crystallization. We have analyzed the $NaMgAl(ox)_3 \cdot 9H_2O$ system again and our results are compared in Table 1 with the early data published by Piper and Carlin.[18] The results are in best agreement with the assumption of *nine* molecules of water of crystallization. It has been noted previously by other researchers that the $P\bar{3}c1$ space group requires a disorder of the water molecules in the nonahydrate.[26] On the basis of the EPR spectra in comparison with the disordered $K_3Al(ox)_3 \cdot 3H_2O$ host it was concluded that the $NaMgAl(ox)_3 \cdot 9H_2O$ system

* To whom correspondence should be addressed. E-mail: h.riesen@adfa.edu.au. Fax:++61 (0)2 6268 80 17.

10.1021/jp020861p CCC: $22.00
Published on Web 08/09/2002

assumes the *P*3c1 space group for which no disorder of the water molecules is required. The present work shows that the nonahydrate exhibits relatively efficient nonphotochemical hole-burning. Properties, such as spontaneous hole-filling etc., are reminiscent of two-level systems (TLSs) encountered in amorphous hosts. TLSs in crystals are usually associated with some disorder.

2. Experimental Section

$NaMgAl(oxalate)_3 \cdot 9H_2O$ and $NaMgCr(oxalate)_3 \cdot 9H_2O$ were prepared as is described in the literature.[18,23] $NaMgAl(oxalate)_3 \cdot 9H_2O$ crystals doped with chromium(III) were grown by slow evaporation from aqueous solutions. The effective chromium(III) concentration of the crystals used in the present work was 4%, as measured by absorption spectroscopy. A 1.5 mm thick crystal was used in the hole-burning experiments.

The samples were cooled by a Janis/Sumitomo SHI-4.5 closed cycle refrigerator capable of reaching 2.5 K. The crystals were mounted on a sapphire window using heat conductive grease (Cry-con).

Luminescence spectra were excited by the 514.5-nm line of an Ar^+ laser (Spectra Physics Stabilite 2017) and the collected emission was dispersed by a monochromator (Spex 1704) equipped with a 1200 grooves/mm holographic grating. Conventional transmission spectra were measured by passing white light through a 694-nm interference filter with a 10-nm bandwith and analyzing the transmitted light with the monochromator.

Spectral holes were measured in transmission by using a single-frequency laser diode (Hitachi HL6738MG). The temperature and current of the laser diode was stabilized and controlled by a Thorlabs LDC500 laser diode driver and a Thorlabs TEC2000 temperature controller in conjunction with a Thorlabs TCLDM9 thermoelectric laser mount. The laser diode had to be operated at 50−60 °C to reach the wavelength of the R-lines. The frequency of the laser was scanned by modulating the current. The modulating waveform was generated by a Stanford SRS DS345 synthesized function generator. In the transient hole-burning experiments, the current, and hence the wavelength, of the laser diode was kept constant for a particular period of time (100 μs −1ms). The current was then modulated by a triangle ramp. The laser diode used in the present experiments could be continuously scanned over ∼40 GHz. The effective line width of the laser was 50 ± 10 MHz as measured by a scanning confocal Fabry-Pérot interferometer (Coherent Model 240 spectrum analyzer with a free spectral range of 1.5 GHz).

The light was detected by a cooled RCA31034C photomultiplier and the photocurrent was converted by a Products-for-Research Model PSA preamplifier. The signal was processed by a lock-in amplifier (EG&G 5210) or a digital storage oscilloscope (Tektronix TDS210).

3. Results and Discussion

Figure 1 presents the nonselectively excited luminescence spectrum of $NaMgAl(oxalate)_3 \cdot 9H_2O$:Cr(III) at 2.5 K. In inset *a* of Figure 1, the absorption and luminescence spectra are compared. The R_1-line in luminescence is slightly shifted to the red in comparison with the absorption spectrum. This shift is indicative of the presence of some excitation energy transfer which can be caused by the reabsorption of emitted photons (radiative process) or a nonradiative mechanism. It is most likely that both mechanisms contribute since the chromium(III) concentration in the present experiments is relatively high (4%). Inset *b* of Figure 1 shows the temperature dependence of the

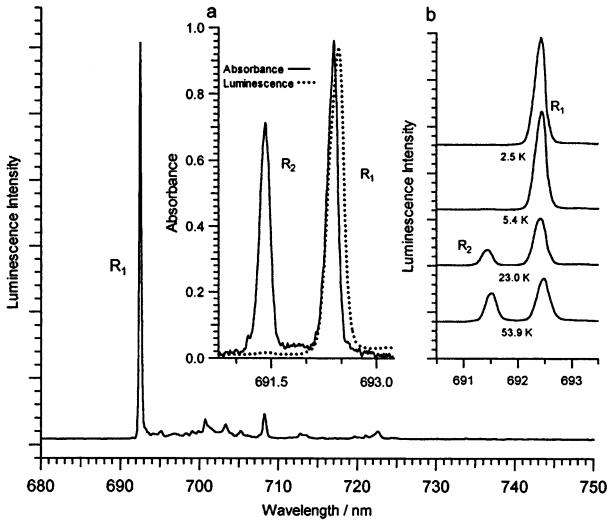

Figure 1. Nonselectively excited luminescence spectrum of $NaMgAl(oxalate)_3 \cdot 9H_2O$:Cr(III) at 2.5 K. The 2.5-K luminescence and absorption spectra in the region of the $^2E \leftarrow {}^4A_2$ electronic origins are compared in inset *a*. Inset *b* illustrates the temperature dependence of the luminescence in the same region.

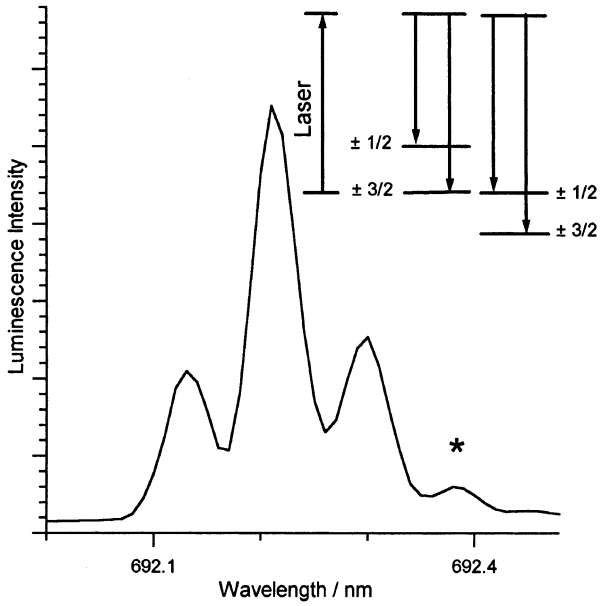

Figure 2. Resonant FLN spectrum of the R_1-line of $NaMgAl(oxalate)_3 \cdot 9H_2O$:Cr(III) at 2.5 K and the associated energy level diagram. The transition marked by an asterisk is due to excitation energy transfer as is discussed in the text.

luminescence spectrum. The intensity of the R_2-line is proportional to the pseudo-Boltzmann population of the upper ^2E level. The ^2E splitting is 20 cm^{-1} and is the result of spin−orbit coupling and the trigonal and rhombic ligand field contributions.

Figure 2 illustrates a 2.5-K resonant FLN experiment in the R_1-line of $NaMgAl(oxalate)_3 \cdot 9H_2O$:Cr(III). The line width is limited by the instrumental resolution of the monochromator. A typical three-line pattern is observed because the chromium(III) centers can have the $R_1(\pm 3/2)$ or the $R_1(\pm 1/2)$ transition (originating from the $\pm 3/2$ or the $\pm 1/2$ spin components of the $^4A_2$ ground state, respectively) in resonance with the laser light. Luminescence occurs to both Kramers doublets leading to the observation of a central resonant line and two equally spaced sidelines. The spacing is given by the zero field splitting (zfs) of the $^4A_2$ ground state. The observed zfs value of 1.6 ± 0.1 cm^{-1} is in agreement with results of EPR and magnetic

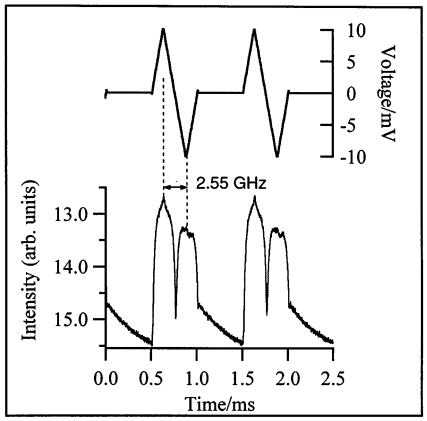

Figure 3. Typical transient spectral hole-burning experiment in the R_1-line of NaMgAl(oxalate)$_3$·9H_2O:Cr(III) at 2.5 K. The voltage ramp, used to modulate the current, is shown in the upper trace. The ±10 mV ramp provides a current modulation of ±0.5 mA which corresponds to a frequency scan of ~2.5 GHz. In the example shown the current of the laser was kept constant at about 76 mA for 0.5 ms; subsequently a triangular ramp was applied in 0.5 ms. The hole was burnt at 692.3 nm with 1 mW of laser light. The hole-burning spectrum is the average of 640 scans.

susceptibility experiments.[21,22] From the latter experiment, it followed that the ±3/2 Kramers doublet is the *very* ground state. From the EPR experiments zfs parameters of $|D| = 0.7786$ cm^{-1} and $|E| = 0.0306$ cm^{-1} were derived. These parameters are defined by the effective spin Hamiltonian of the $^4A_2$ ground state as is given by eq 1

$$H = D[S_z^2 + S(S+1)] + E(S_x^2 - S_y^2) \qquad (1)$$

The nonzero value of E implies the presence of a lower-symmetry ligand field.

The transition marked with an asterisk in the inset of Figure 2 is due to excitation energy transfer. Centers that have the R_1-(±3/2) transition in resonance with the laser can emit resonantly via the R_1(±3/2)-line or nonresonantly via the R_1(±1/2)-line. The latter transition can coincide with the R_1(±3/2)-line of other chromophores within the inhomogeneous distribution providing a pathway for radiative or nonradiative excitation energy transfer. These centers can reemit at the same wavelength or by the R_1(±1/2)-line, shifted to lower energy by the $^4A_2$ zfs of 1.6 cm^{-1} (transition marked by an asterisk).

A typical transient hole-burning (THB) spectrum is shown in Figure 3. The current of the laser diode, and hence the wavelength, is kept constant for a particular time; subsequently it is scanned by applying an external voltage ramp to the laser diode controller. The ±10 mV triangle ramp in Figure 3 translates to a current variation of ±0.5 mA which corresponds to a frequency scan of ~2.5 GHz. To verify the transient nature of the holes we have also performed experiments where the burn period (constant current) is followed by several scans. This is illustrated in Figure 4 where the hole depth is compared with the single-exponential $I=I_0\exp(-t/T_1)$ which describes the decay of the excited state with a lifetime of $T_1 = 0.90$ ms. We notice that the holes decay *slightly* faster than predicted by the decay curve. This indicates that *nonradiative* excitation energy transfer to chromophores with different transition energies occurs in the lifetime of the excited state.

The observed width depends both on the depth and the delay time of the readout of the hole. Figure 5 shows a very shallow hole (~1% change in optical density). Correcting for the laser line width, $\Gamma_{laser} = 50$ MHz, using eq 2 we could observe holes

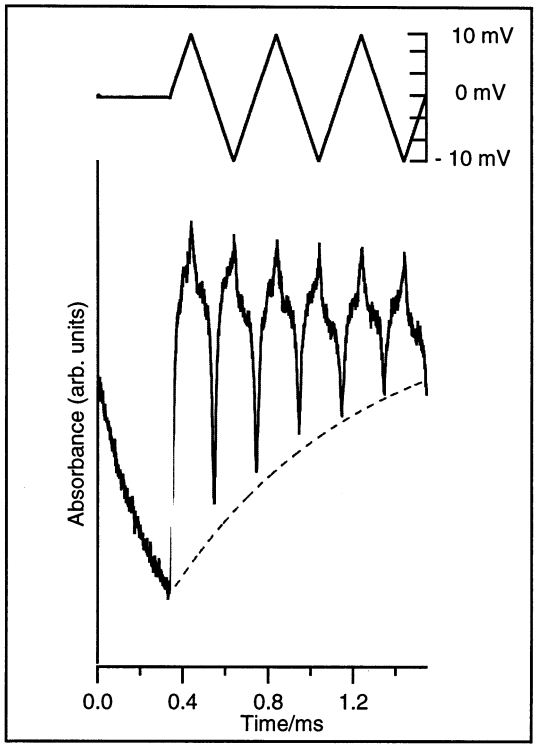

Figure 4. Illustration of the transient nature of a 5% deep spectral hole burnt into the R_1-line of NaMgAl(oxalate)$_3$·9H_2O:Cr(III) at 2.5 K and 692.4 nm. The waveform generator provides multiple scans; the hole is read out 5 times at intervals of 200 μs after a burn period of 330 μs. The dashed line is the calculated decay curve, $I=I_0\exp(-t/T_1)$, with $T_1 = 0.9$ ms. The hole-burning spectrum is the average of 640 scans.

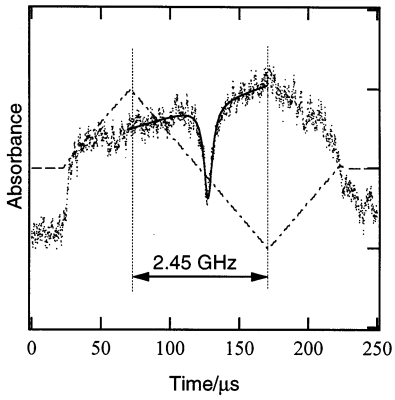

Figure 5. Shallow (ΔOD = 1%) transient spectral hole in the R_1-line of NaMgAl(oxalate)$_3$·9H_2O:Cr(III) at 2.5 K. The solid line is a Lorentzian with a width $\Gamma = 180$ MHz. The hole-burning spectrum is the average of 1280 scans.

with a width of ~90 MHz at 2.5 K.

$$\Gamma_{hole} \approx 2\Gamma_h + \sqrt{2}\Gamma_{laser} \qquad (2)$$

The temperature dependence of the transient spectral hole is summarized in Figure 6. The data in this figure were collected under ideal conditions that is to say short burn (200 μs) and delay time (200 μs).

Neglecting power broadening the line width of an electronic transition is given by eq 3

$$\Gamma_h = \frac{1}{\pi T_2} \qquad (3)$$

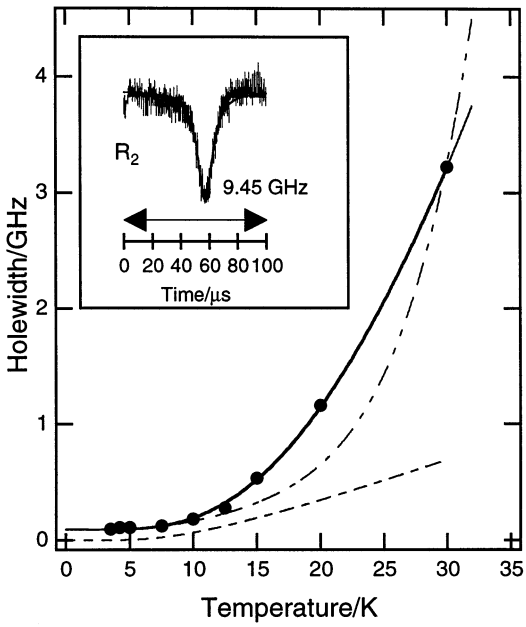

Figure 6. Temperature dependence of the width of a transient spectral hole burnt into the R_1-line of $NaMgAl(oxalate)_3 \cdot 9H_2O$:Cr(III) at 692.22 nm. The burn and scan times were 200 μs each. The inset shows a transient hole burnt into the R_2-line at 691.45 nm with a fitted Lorentzian ($\Gamma = 1.19$ GHz). The dashed line is the contribution to the R_1 holewidth by the direct process as calculated from the R_2 holewidth, $\Gamma_{direct} = 1.12\bar{n}(20\ cm^{-1})$. The dash−dot line shows the temperature dependence predicted by the sum $\Gamma = \Gamma_0 + \Gamma_{direct} + \Gamma_{Raman}$ using eq 6 for Γ_{Raman} and the solid line is the calculated sum using eq 8 for Γ_{Raman}. The experimental data has been corrected for the laser line width of 50 MHz.

where the effective dephasing time T_2 is determined by the lifetime of the excited state, T_1, and the pure dephasing time T_2*.

$$\frac{1}{T_2} = \frac{1}{2T_1} + \frac{1}{T_2^*} \tag{4}$$

The pure dephasing time is strongly temperature dependent. In the present system we have to consider two contributions to the holewidth of the R_1-line. First, the direct process to the upper ^2E level is thermally activated. To calculate this contribution we have performed transient spectral hole-burning experiments on the R_2 transition. A transient spectral hole in this higher-energy transition is illustrated in the inset of Figure 6. The holewidth of 1.12 GHz at 2.5 K (corrected for the 50 MHz laser line width) directly measures the lifetime of the R_2 level. To our knowledge this is the first report of transient hole burning in the R_2-line of a chromium(III) system. At 2.5 K, pure dephasing is relatively slow and the dominant contribution to the holewidth of the R_2-line is by the direct process reflected in T_1. By using eq 3 we then evaluate $T_1(R_2) = 284$ ps. This lifetime lies somewhere between the reported values for ruby (~1 ns) and $[Rh(bpy)_3](PF_6)_3$:Cr(III) (~3 ps).[27,28] This can be expected since the ^2E splitting in the three systems is comparable but the density of phonon states at 20−30 cm^{-1} increases in the order Al_2O_3:Cr(III) < $NaMgAl(oxalate)_3 \cdot 9H_2O$:Cr(III) < $[Rh(bpy)_3](PF_6)_3$:Cr(III). The direct process from the R_1 to the R_2 level requires the absorption, and hence the presence, of 20 cm^{-1} phonons. Thus, the temperature dependence of its contribution to the line width can be calculated by using eq 5

$$\Gamma_{direct}(R_1) = \frac{1}{2\pi T_1(R_2)}\,\bar{n}(\Delta E) \tag{5}$$

where $\bar{n}(\Delta E) = 1/[\exp(\Delta E/k_B T) - 1]$ with $\Delta E = 20\ cm^{-1}$.

Second, the contribution by the two-phonon Raman scattering process can become dominant at higher temperatures. When the quadratic electron−phonon coupling is weak the contribution to the holewidth (line width) by this process can be described by the perturbative expression 6[29]

$$\Gamma_{Raman} \propto \int_0^\infty \rho(\omega)^2 \bar{n}(\omega)[\bar{n}(\omega) + 1]d\omega \tag{6}$$

where $\rho(\omega)$ is the weighted density of phonon states. If the Debye approximation is used for the density of phonon states in eq 6, the famous T^7 temperature dependence for the Raman process results.[30] The density of phonon states can also be approximately determined by the intensity, $I(\omega)$, of vibrational sidelines in the luminescence spectrum by using eq 7[29]

$$I(\omega) \propto \frac{\rho(\omega)}{\omega^2} \tag{7}$$

The angular frequency ω is measured relative to the electronic origin.

The $[Cr(oxalate)_3]^{3-}$ anion is a distinct unit in the present system. Hence, the vibrations which couple to the electronic states of the molecular anion are best described as pseudolocal. If the frequency and lifetime of the pseudolocal modes in the ground electronic state are given by $\omega_0 i$ and $\tau_0 i$, respectively, and their product $\tau_0 i \omega_0 i \gg 1$ eq 6 can be approximated by[31−35]

$$\Gamma_{Raman} \approx \sum\nolimits_i a_i \bar{n}(\omega_0{}^i)[\bar{n}(\omega_0{}^i) + 1] \tag{8}$$

where a_i are coupling constants.

In Figure 6, the holewidth data is analyzed by eq 9

$$\Gamma(T) = \Gamma_0 + \Gamma_{direct} + \Gamma_{Raman} \tag{9}$$

employing either eq 6 or 8 for the Raman term. Γ_0 is the residual holewidth for temperatures approaching 0 K; it can contain both homogeneous and heterogeneous contributions.[36]

It appears that the temperature dependence is not well described when the integral eq 6 is applied. However, a very good approximation is obtained by taking into account two pseudolocal phonons for the Raman term given by eq 8 with experimentally determined frequencies of 33.3 and 52.3 cm^{-1} and fitted coupling constants of $a_1 = 3.2$ and $a_2 = 14.9$.

Nonsymmetric low-frequency vibrations of the $[Cr(oxalate)_3]^{3-}$ molecular anion may substantially alter the trigonal and/or rhombic ligand field. Consequently, it can be expected that such modes may be very effective in dephasing the electronic wave functions. If eq 6 is used in conjunction with an effective density of phonon states as determined from the vibrational sidelines in the luminescence spectrum the contribution by these low energy modes may be underestimated.

A relatively high chromium(III) concentration of 4% (~8 10^{19} $[Cr(ox)_3]^{3-}/cm^3$) was used in the present experiments. We have recently measured spectral holes in the $R_1(\pm 1/2)$ transition of a 0.5% crystal using a pseudo-external cavity laser and found a holewidth of ~20 MHz at 2.5 K in zero field.[37] This concentration dependence indicates that the residual holewidth in the present sample of $\Gamma_0 = 93$ MHz is governed by chromium(III)−chromium(III) spin−spin interactions.[36,38] To a lesser extent superhyperfine interactions with the ^{27}Al nuclear spin, $I = 5/2$, of the surrounding $[Al(oxalate)_3]^{3-}$ complexes and the proton spin of the water molecules may also contribute to the line width.[37]

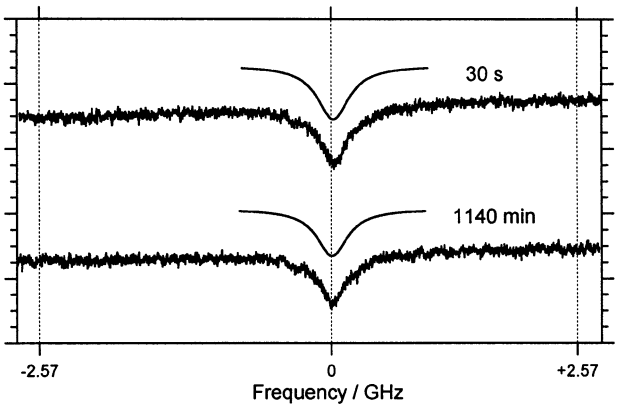

Figure 7. Persistent spectral hole burnt into the R_1-line of NaMgAl-(oxalate)$_3$·9H$_2$O:Cr(III) at 2.5 K. The hole was burnt with 1 mW of 692.24 nm laser light for 20 min and subsequently measured with a delay of 30 s and 1140 min. The initial hole depth was ∼1%.

We note here that the direct process between the ±3/2 and ±1/2 spin components of the $^4A_2$ ground state will also contribute to the (residual) holewidth. In a Debye approximation of the density of phonon states this process is expected to be ∼2000 times slower than the $R_2 \rightarrow R_1$ relaxation and thus this contribution is of the order of magnitude of 0.5 MHz.

The R_1 transition of NaMgAl(oxalate)$_3$·9H$_2$O:Cr(III) exhibits persistent spectral hole-burning. This is illustrated in Figure 7 which shows an ∼1% deep spectral hole burnt into the R_1 line at 692.24 nm for 20 min at 2.5 K. The hole was measured 30 s and 1140 min after the burn period. Taking into account the 50 MHz laser line width, Γ_{laser}, the hole widths, Γ_{hole}, are 260 ± 20 MHz and 280 ± 20 MHz. The hole broadening over this extended period of time has an order of magnitude of only 20 MHz. Consequently, spectral diffusion is not significant on the minute time scale in the present system. The hole area is reduced by about 15 % after the 1140 min period implying that spontaneous hole filling is rather slow at this temperature, however, it is thermally activated. For example, if a hole is initially burnt at 2.5 K and subsequently the sample temperature is cycled to 30 K for 600 s, only 30% of the original hole area remains at 2.5 K; raising the temperature to 45 K for 120 s reduces the hole area to 8%; if the temperature is raised to 60 K the hole is completely erased in a few seconds. The temperature dependence of the spontaneous hole-filling is symptomatic of TLSs in a crystal.[39]

The holes can also be erased by exciting the sample into the $^4T_2 \leftarrow {}^4A_2$ transition with 50 mW of 514.5 nm Ar^+ light for a few seconds. This, together with the erasure of holes at elevated temperatures, indicates that the hole-burning mechanism is nonphotochemical. Support for this assignment stems from the observation that the integrated absorbance of the R-lines is invariant to multiple hole-burning. Furthermore, the system exhibits no photochemistry upon laser excitation into the $^4T_2$ transition. Thus, the "photoproduct" lies within the inhomogeneous distribution.

A variation of some hydrogen bond between crystalline water molecules and the oxalate ligands is a likely origin of the nonphotochemical hole-burning mechanism. To investigate this possibility we have burnt a spectral hole into the R_1-line of the NaMgAl(ox)$_3$·8H$_2$O:Cr(III) system. Previous work has shown that the 9th water molecule in NaMgAl(ox)$_3$·9H$_2$O can be reversibly removed at 98 °C without causing significant variations in the optical or macroscopic qualities of the crystal.[21,24,40] It has been suggested that the water molecule can move in to and out of the crystal through some channels within the structure.[21] Upon the removal of the water molecule the ^2E splitting collapses from 20 cm^{-1} to ∼3 cm^{-1} and the R_1-line shifts to 690.8 nm.[40] We have burnt holes in the nona- and octahydrate under the same conditions as is illustrated in Figure 8. It appears that the hole-burning efficiency is drastically reduced by the removal of one water molecule. Thus, the efficient nonphotochemical hole-burning observed for the nonahydrate is most likely caused by hydrogen-bonding of the water molecule with the oxalate ligand.

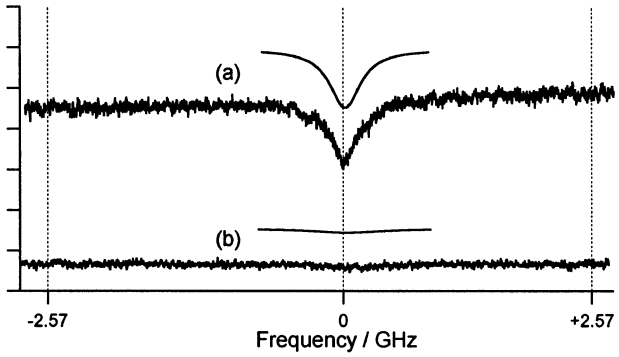

Figure 8. Comparison of spectral hole-burning of the R_1-line in the NaMgAl(ox)$_3$·9H$_2$O:Cr(III) and NaMgAl(ox)$_3$·8H$_2$O:Cr(III) systems at 2.5 K. The samples were exposed to the same burn fluence.

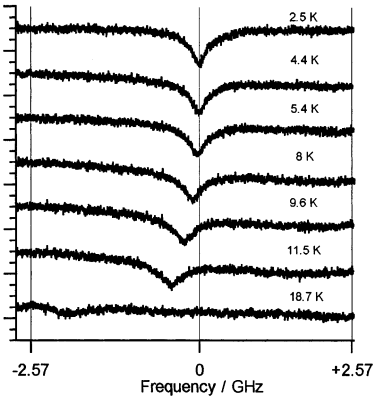

Figure 9. Temperature dependence of a persistent spectral hole burnt into the R_1-line of NaMgAl(oxalate)$_3$·9H$_2$O:Cr(III) at 692.25 nm and 2.5 K.

The temperature dependence of a persistent spectral hole burnt into the R_1-line of NaMgAl(oxalate)$_3$·9H$_2$O:Cr(III) at 2.5 K is illustrated in Figure 9. The hole was burnt with 1 mW of 692.25 nm laser light for 20 min and the initial hole depth was ∼1%. After each measurement the temperature was lowered back to 2.5 K and the hole was remeasured. The 2.5-K holewidth remained constant after each temperature cycle and hence spectral diffusion on the minute time scale is insignificant in the investigated temperature range. Upon increasing the temperature, the spectral hole broadens and shifts to the red. The same experiment was performed on a persistent spectral hole burnt into the R_2-line. Some representative spectra are shown in Figure 10.

In the weak coupling limit the temperature-dependent shift of the electronic origin by two-phonon Raman processes can be described by the perturbative expression 10[9,31]

$$\delta E_{\text{Raman}} \propto \int_0^\infty \rho(\omega)\bar{n}(\omega)d\omega \qquad (10)$$

When the Debye approximation is employed in eq 10 for the density of phonon states the widely reported T^4 temperature

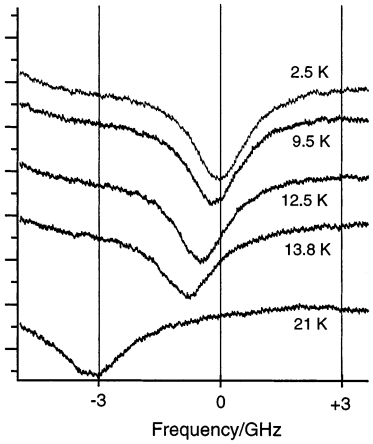

Figure 10. Temperature dependence of a persistent spectral hole burnt into the R_2-line of NaMgAl(oxalate)$_3$·9H$_2$O:Cr(III) at 691.45 nm and 2.5 K.

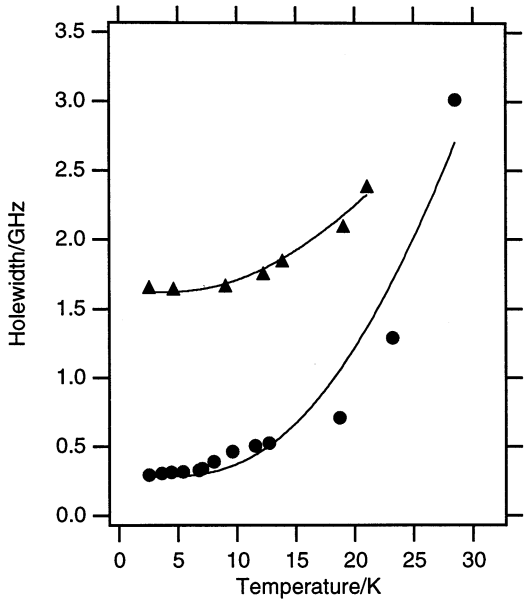

Figure 11. Summary of the temperature dependence of the width of persistent spectral holes burnt into the R_1 and R_2-lines of NaMgAl(oxalate)$_3$·9H$_2$O:Cr(III) at 1.5 K. The solid lines were calculated by using eq 9 where the Raman term was approximated by eq 8 with the parameters $\omega_1 = 33.3$ cm^{-1}, $\omega_2 = 52.3$ cm^{-1}; $a_1 = 2.6$, $a_2 = 12.9$ for R_1 and $a_1 = 2.5$, $a_2 = 12.4$ for R_2. Data were corrected for the laser line width.

dependence is predicted.[30] Again, if we restrict the model to pseudolocal modes eq 10 simplifies to[33]

$$\delta E_{\text{Raman}} = \sum_i b_i \bar{n}_i(\omega) \qquad (11)$$

In Figures 11 and 12 we have analyzed the temperature dependence of persistent spectral holes in the R-lines by using the eqs 5−11. In the analysis of the temperature dependence of the width, the ratio of a_1/a_2 was kept at a value of 0.21 as determined in the transient spectral hole-burning experiments. For the R_2 line, the contribution to the width by the direct process is given by eq 12 because this process involves the emission of a phonon and hence is possible at $T = 0$ K

$$\Gamma_{\text{direct}}(R_2) = \frac{1}{2\pi T_1(R_2)} [\bar{n}(\omega) + 1] \qquad (12)$$

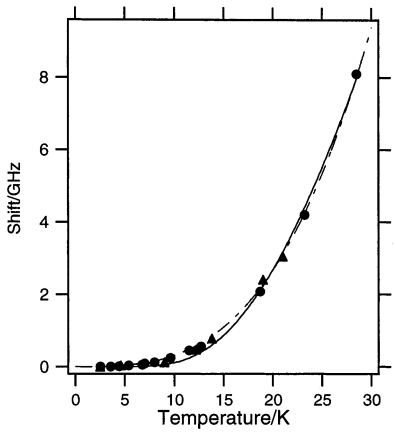

Figure 12. Summary of the temperature dependence of the shift of persistent spectral holes burnt into the R_1 (full circles) and R_2 (full triangles) lines of NaMgAl(oxalate)$_3$·9H$_2$O:Cr(III) at 2.5 K. The dashed line has been calculated by using eq 10 with a density of phonon states determined from the vibrational sidelines in the luminescence spectrum. The solid line has been calculated by using eq 11 with $\omega_1 = 33.3$ cm^{-1}, $\omega_2 = 52.3$ cm^{-1}, $b_1 = 7.7$, $b_2 = 81.3$.

The fitted values for the coupling parameters are reasonably close to the ones obtained in the transient hole-burning experiment. Furthermore, within the standard deviation, they are the same for both R-lines. The determined residual hole-widths $\Gamma_0(R_1) = 260$ MHz and $\Gamma_0(R_2) = 1.63$ GHz are significantly larger than in the transient hole-burning experiments for both lines. The two experiments are performed on the μs-ms and minute time scale, respectively. Spectral diffusion is a likely cause for the larger widths of the persistent holes.

To measure the broadening of the hole by spectral diffusion various burn periods and lengths of the triangle ramp were applied in the *transient* hole-burning experiments. The transient spectral hole shows a broadening of 30 ± 10 MHz from 0.2 ms (burn and read time) to 1.2 ms (30 GHz/s). This result has to be compared with the spectral diffusion observed in the persistent holes of $\sim 3 \times 10^{-4}$ MHz/s on the minute time scale. It is obvious that spectral diffusion is much slower at long times and the behavior can be described by a logarithmic law. However, more data points between 1 ms and 1 s are needed to assign any particular function to the time behavior. It is possible that the spectral diffusion on the μs−ms time scale is governed by electronic (and nuclear) spin-flips whereas the long time behavior may be associated with TLSs of the water molecules responsible for the hole-burning mechanism.

4. Conclusions

By using transient and persistent spectral hole-burning in the $^2E \leftarrow {}^4A_2$ transitions of NaMgAl(ox)$_3$·9H$_2$O:Cr(III) we have been able to demonstrate that pseudolocal vibrations are mainly responsible for the temperature dependence of the dephasing of the ^2E levels and their energy shift. The residual line width of 46 MHz is dominated by chromium(III)−chromium(III) electron spin−spin interactions but may also contain contributions by superhyperfine interactions with the ^{27}Al and ^{1}H nuclear spins. This is currently the subject of investigation by the application of external magnetic fields.

The NaMgAl(ox)$_3$·9H$_2$O:Cr(III) system exhibits nonphotochemical hole-burning, a rare phenomenon in crystalline systems. The hole-burning mechanism appears to be based on the rearrangement of some water molecule of hydration. It seems likely that many other inorganic systems, containing water molecules of crystallization, may exhibit persistent nonphoto-

chemical hole-burning in electronic transitions. This may enable the chemist to optimize the hole-burning efficiency by tailoring compounds. We note here that the present work is related to the elegant infrared hole-burning studies of water molecules in Tutton salts.[41]

Spontaneous hole-filling in $NaMgAl(ox)_3 \cdot 9H_2O$:Cr(III) is thermally activated and spectral diffusion on the minute time scale is relatively slow in the investigated temperature range of 2.5−30 K.

The present study shows that there is a great potential for the application of inexpensive laser diodes in the spectroscopy of coordination compounds. For example, due to the inherent properties of diode lasers it is possible to measure very shallow holes with extremely good signal-to-noise ratios. Furthermore, the wavelength of laser diodes can be rapidly scanned, enabling elegant transient hole-burning studies.

Acknowledgment. Financial support of this work by the large grant scheme of the Australian Research Council (Grant No. A00104371) is gratefully acknowledged. We would also like to thank J. Hughes for his assistance in the later stage of this project. K. Piper and K. Richens are acknowledged for their technical support.

References and Notes

(1) *Persistent Spectral Hole-Burning: Science and Applications*; *Topics in Current Physics Volume 44*; Moerner, W. E., Ed.; Springer-Verlag: Heidelberg, 1988.

(2) *Laser Spectroscopy of Solids, Applied Physics, Vol. 49*; Yen, W.; Selzer, P. M., Eds.; Springer-Verlag: Berlin, 1981.

(3) Völker, S. *Annu. Rev. Phys. Chem*. **1989**, *40*, 499.

(4) Friedrich, J.; Haarer, D *Angew. Chem., Int. Ed. Engl.* **1984**, *23*, 113.

(5) MacFarlane, R. M.; Shelby, R. M. In *Spectroscopy of Solids Containing Rare Earth Ions*; Kaplyanskii, A. A.; Macfarlane, R. M., Eds.; Elsevier Science Publishers: Amsterdam, 1987; pp 51−184.

(6) Krausz, E.; H. Riesen, H. In *Inorganic Electronic Structure and Spectroscopy*; Lever, A. P. B., Solomon, E. I., Eds.; John Wiley & Sons: New York, 1999; Vol. I., pp 307−352.

(7) Gorokhovskii, A. A.; Kaarli, R. K.; Rebane, L. A. *JETP Lett*. **1974**, *20*, 216.

(8) Kharlamov, B. M.; Personov, R. I.; Bykovskaya, L. A. *Opt. Commun*. **1974**, *12*, 191.

(9) Szabo, A. *Phys. Rev. B* **1975**, *11*, 4512.

(10) Liu, G. K.; Li, S. T.; Beitz, J. V. *J. Lumin*. **1999**, *83 & 84*, 343.

(11) Boye, D. M.; Macfarlane, R. M.; Sun, Y.; Meltzer, R. S. *Phys. Rev. B* **1996**, *54*, 6263.

(12) Holliday, K.; N. B. Manson, N. B. *J. Phys.: Condens. Matter*, **1989**, *1*, 1339.

(13) Reeves, R. J.; Macfarlane, R. M. *J. Opt. Soc. Am.*, **1992**, *B 9*, 763.

(14) Macfarlane, R. M.; Reeves, R. J.; Jones, G. D. *Opt. Lett*, **1987**, *12* 660.

(15) Riesen, H.; Bursian, V. E.; Manson, N. B. *J. Lumin.* **1999**, *85*, 107.

(16) Reinot, T.; Small, G. J. *J. Chem. Phys.* **2001**, *114*, 9105.

(17) Hayes, J. M.; Small, G. J. *Chem. Phys.* **1978**, *27*, 151.

(18) Piper, T. S.; Carlin, R. L. *J. Chem. Phys.***1961**, *35*, 1809.

(19) Mortensen, O. S. *J. Chem. Phys.* **1967**, *47*, 4215.

(20) Coleman, W. F.; Forster, L. S. *J. Lumin.* **1971**, *4*, 429.

(21) Bernheim, R. A.; Reichenbecher, E. F. *J. Chem. Phys.* **1969**, *51*, 996.

(22) Lahiry, S.; Kakkar, R. *Chem. Phys. Lett.* **1982**, *88*, 499.

(23) Frossard, L. *Schweiz. Mineral. Petrog. Mitt.* **1956**, *35*, 1.

(24) Zbieranowski, W. T., *Chem. Phys. Lett.* **1975**, *36*, 166.

(25) Suh, J.-S.; Shin, J.-Y.; Yoon, C.; Lee, K.-W.; Suh, I.-H.; Lee, J.-H.; Ryu, B.-Y.; Lim, S.-S. *Bull. Korean Chem. Soc.* **1994**, *15*, 255.

(26) Doetschman, D. C.; McCool, B. J. *Chem. Phys.* **1975**, *8*, 1.

(27) Rives, J. E.; Meltzer, R. S. *Phys. Rev. B* **1977**, *16*, 1808.

(28) Riesen, H. *J. Lumin.* **1992**, *54*, 71.

(29) Imbusch, G. F.; Yen, W. M.; Schawlow, A. L.; McCumber, D. E.; Sturge, M. D. *Phys. Rev.* **1964**, *133*, A1029.

(30) McCumber, D. E.; Sturge, M. D. *J. Appl. Phys.* **1963**, *34*, 1682.

(31) Hsu, D.; Skinner, J. L. *J. Chem. Phys.* **1985**, *83*, 2107.

(32) Sapozhnikov, M. N. *Phys. Stat. Sol. B* **1976**, *75*, 11.

(33) Freiberg, A.; Rebane, L. A. *Phys. Stat. Sol. B* **1977**, *81*, 359.

(34) Osad′ko, I. S. In *Spectroscopy and Excitation Dynamics of Condensed Molecular Systems*, Agranovich, V. M.; Hochstrasser, R. M., Eds.; North Holland: Amsterdam, 1983; pp 437−514.

(35) Glasbeek, M.; Smith, D. D.; Perry, J. W.; Lambert, Wm. R.; Zewail, A. H. *J. Chem. Phys*. **1983**, *79*, 2145.

(36) Szabo, A.; Kaarli, R. *Phys. Rev. B* **1991**, *44*, 12307.

(37) Hughes, J. L.; Riesen, H., unpublished results.

(38) Szabo, A.; Muramoto, T.; Kaarli, R. *Phys. Rev. B* **1990**, *42*, 7769.

(39) Murray, T. A.; Holliday; K., Manson, N. B. *J. Lumin.* **2001**, *94*−*95*, 683.

(40) Schönherr, T.; Spanier, J.; Schmidtke, H.-H., *J. Chem. Phys.* **1989**, *93*, 5969.

(41) Fei, S.; Strauss, H. L. *J. Phys. Chem.* **1996**, *100*, 3414.